

H13-25

EFFECTS OF NOCTURNAL THERMAL CIRCULATION AND BOUNDARY LAYER STRUCTURE ON POLLUTANT DISPERSION IN AREAS OF COMPLEX TERRAIN

Mireia Udina¹, Maria Rosa Soler¹ and Raúl Arasa¹¹Department of Astronomy and Meteorology, University of Barcelona, Barcelona, Spain

Abstract: Air quality models are highly sensitive to atmospheric numerical models, which depend critically on the lower boundary conditions, mainly under strongly thermally-stratified conditions. In these situations, the determining factors are turbulent kinetic energy and surface layer parameterizations. In this study, two meteorological mesoscale models, MM5 and WRF, which use different planetary boundary layer (PBL) schemes, were run in very stable conditions over the Duero basin in the Iberian Peninsula. The models were compared, checked against available information, and coupled to the CMAQ model to analyze the influence of the boundary layer parameterizations on air pollutant distribution and concentration.

Key words: Mesoscale models; Nocturnal boundary layer parameterizations; Air quality.

1. INTRODUCTION

Mesoscale systems and related circulatory patterns exert a great influence on the transport and diffusion of atmospheric pollutants. However, understanding the processes controlling this influence, particularly during the night-time, is very complex and there are still many problems to solve, as the correct representation of atmospheric pollutant transport requires a good knowledge of the flow structure associated with the mesoscale system and the corresponding boundary layer. Most pollutants are emitted in this layer and the interaction between the two scales is strong.

In mountain areas, mesoscale systems that are forced by night-time temperature gradients are the mountain and valley breeze regimes, which include both drainage and down-valley winds (Whiteman, 2000). As the impact of the planetary boundary layer (PBL) scheme is very important in air quality modelling, we examine the performance of the PBL schemes implemented in the Weather Research and Forecasting (WRF-ARW) model (Skamarock *et al.*, 2008) to simulate these topographic winds. This is achieved by comparisons with simulations carried out with the MM5 model (Grell *et al.*, 1994) in the same study area and checked against available information. The model was run over the Duero basin in the Iberian Peninsula using high vertical numerical resolution to capture low-level flow details. To analyze the dispersion patterns caused by these down-valley flows, we considered several scenarios, which were obtained by placing a virtual source over the Duero basin. Pollutant dispersion results obtained by coupling the photochemical model CMAQ (Byun and Chang 1999) to MM5 and WRF models showed the influence of PBL schemes on air pollutant distributions and concentrations.

2. EXPERIMENTAL DESIGN AND NUMERICAL MODEL DESCRIPTION

2.1 Area characteristics and data used

The study area covers the northern Castillian plateau (Spain), which is the basin of the Duero River. This plateau is surrounded by high mountain ranges that peak at about 2000 m above sea level: the Cantabrian range to the north, the Iberian range to the east, and the Central range to the south. To the west, there are a number of minor ranges that close the plateau. The Duero River flows out through a very narrow passage to Portugal and the Atlantic Ocean. The basin has a gentle slope from the foothills towards the Duero River (Figure 1). On the central part of the northern Castillian plateau, there is a secondary plateau (Montes Torozos, 800 km²) at 840 m above sea level. It is surrounded by prairies covered by low density grass or land used for cereal cultivation. The Torozos are flat and about 50 m higher than the wide plains of the surrounding plateau. They have a gentle slope of 30 m along a 50 km stretch from the north-east to the south-west, while the north-west and south-east borders are slightly higher than the level of the inner plateau.

The data used to verify the simulations were taken from the 100 metre tower of the CIBA (*Centro de Investigacion de la Baja Atmósfera*) site, which is located in the central area of Montes Torozos (Bravo *et al.*, 2008). The data selected from the CIBA database of the 100 metre tower refer to five levels that measure wind velocity at 2.2, 9.6, 34.6, 74.6 and 98.6 m AGL, wind direction at 9.6, 34.6, 74.6 and 98.6 m AGL, temperature at 2.3, 10.5, 20.5, 35.5 and 97.5 m AGL, and two levels of moisture at 10 and 97 m AGL. In addition, the CIBA tower measures turbulent fluctuations of wind and virtual temperature with sonic anemometers at four levels: 5.6, 19.6, 49.6 and 96.6 m AGL. With this dataset, we could check the model output for one column up to 100 metres. The mean values and the turbulent fluxes that are parameterized in the models can be compared at many points of the vertical grid for this gridbox.

2.2 Meteorological characteristics of the simulation period

After a careful inspection of synoptic conditions and satellite images, a three-day sequence (13-15 January 2003) was chosen for the analysis, with a high-pressure system over the basin that led to extremely weak winds on the last night: at 100 m AGL at the CIBA site they were about 2 ms⁻¹. We focused the study on this second night (14-15), which corresponds to a typical stable night with clear skies, weak winds and strong nocturnal radiation inversions that favour the development of mesoscale circulation, such as drainage winds, valley winds and low level jets, as well as intermittent turbulence episodes.

2.3 Numerical model configurations

Meteorological numerical simulations were performed using WRF-ARW Version 3.1.1 and the PSU/NCAR mesoscale model, MM5 Version 3.7. Both models were configured with two nested domains and grids of 5 and 1 km respectively (Fig. 1). One-way nesting was used for the smaller domain. The outer domain covered 150x100 grid cells in the entire Duero basin and some surrounding areas, and the inner domain covered 160x101 grid cells in the area around the CIBA site in the centre

of the basin. The vertical grid was common to both domains, with 86 vertical levels and a resolution of 3 m close to the surface, which decreased gradually with height, thus enabling low level flow details to be captured. The domain top was at 100 hPa. Initial and boundary conditions were updated every six hours with information obtained from the European Centre for Medium Range Weather Forecasting (ECMWF) model, with a 1.5°x1.5° resolution.

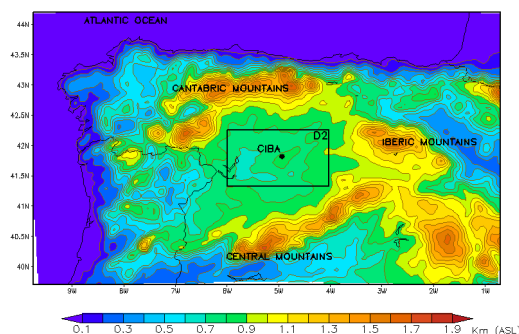


Figure1. Topography of the studied area (0.1 km contours), location of the CIBA site and modelling domains

Three sets of model experiments were designed to explore the accuracy of the nocturnal boundary layer predictions as a function of turbulence physics. The first experiment used MM5 with the physical options presented in Table 1, including the ETA scheme for the PBL. The second and third experiments (WRF experiments), using similar MM5 physical options, explored PBL sensitivities by comparing solutions using the WRF’s standard versions of the Mello-Yamada-Janjic (MYJ) scheme (Janjic, 2002) and the newer Quasi-Normal Scale Elimination turbulence scheme (QNSE) (Sukoriansky *et al.*, 2006). For very stable conditions, stability can be so high that the turbulence collapses (flow effectively becomes laminar). However, in a model, at least some mixing is required to maintain numerical stability and to avoid the phenomena of “runaway” surface cooling, which is generally specified through one or more constant parameters. Since the QNSE scheme in WRF borrows much of its code from the MYJ 1.5-order TKE-predicting scheme, both turbulence parameterizations contained similar minimum parameters: a background value of turbulent kinetic energy, TKE_{MIN} , and a limiting length scale, l_b . However, as shown in Table 2, while the QNSE scheme used the same l_b as MYJ, the TKE_{MIN} in QNSE was an order of magnitude smaller. For the MM5 model, the background value of turbulent kinetic energy was set to $0.2 \text{ m}^2\text{s}^{-2}$.

Table 1. Physical options in MM5 and WRF models

Physics	MM5	WRF-MYJ	WRF-QNSE
Microphysics	Reisnel graupel (Reisner2)	New Thompson	New Thompson
Atmospheric Radiation	Cumulus radiation scheme	Short wave:Dudhia Long wave:RRTM	Short wave:Dudhia Long wave:RRTM
Surface Layer	ETA similarity (Monin Obukhov)	ETA similarity (Monin Obukhov)	ETA similarity (Monin Obukhov)
Land Surface	Noah Land-Surface Model	Noah Land-Surface Model	Noah Land-Surface Model
Planetary Boundary Layer	ETA scheme $TKE_{MIN}= 0.2 \text{ m}^2\text{s}^{-2}$	Mellor-Yamada-Janjic (MYJ)-ETA scheme $TKE_{MIN}= 0.1 \text{ m}^2\text{s}^{-2}$	Quasi-Normal Scale Elimination (QNSE) $TKE_{MIN}= 0.01 \text{ m}^2\text{s}^{-2}$
Cumulus	Grell	Grell 3D	Grell 3D

The photochemical model used in this study to simulate pollutant dispersion is the U.S. EPA model-3/CMAQ model. This model, which is supported by the U.S. Environmental Protection Agency (EPA), is continuously being developed. CMAQ Version 4.6 simulations utilize the CB-05 chemical mechanism and associated EBI solver, including gas phase reactions involving N_2O_5 and H_2O . They also remove obsolete mechanism combinations (e.g. gas+aerosols w/o). In addition to these changes, Version 4.6 includes various modifications to the aerosol module (AERO4). No initial and boundary conditions are considered for the CMAQ model in these simulations, in order not to mask the emission transport of the specific virtual source considered in this study.

3. METEOROLOGICAL MODEL RESULTS AND EVALUATION

The results are presented in two main sections. First, we compare the models and discuss the flow patterns near the ground. Then, we compare the results for the model columns that correspond to the CIBA site with the 100 m tower data, including the temporal evolution.

3.1 Flow patterns

On a very stable night, flow patterns are likely to be dominated by thermally driven flows. All models forecast downslope drainage winds from the Cantabrian, Iberian and Central mountain ranges in the bigger domain. There were no significant differences between the models. However, major differences were observed in the vicinity of the steep terrain. As the inner domain has 1 km resolution, model comparisons and evaluations were focussed on this domain. Figure 2 shows this behaviour by comparing wind pattern simulations at 10 m and 0400 UTC in the inner domain for the MM5 (a) and the WRF model using MYJ and QNSE schemes (b and c) respectively.

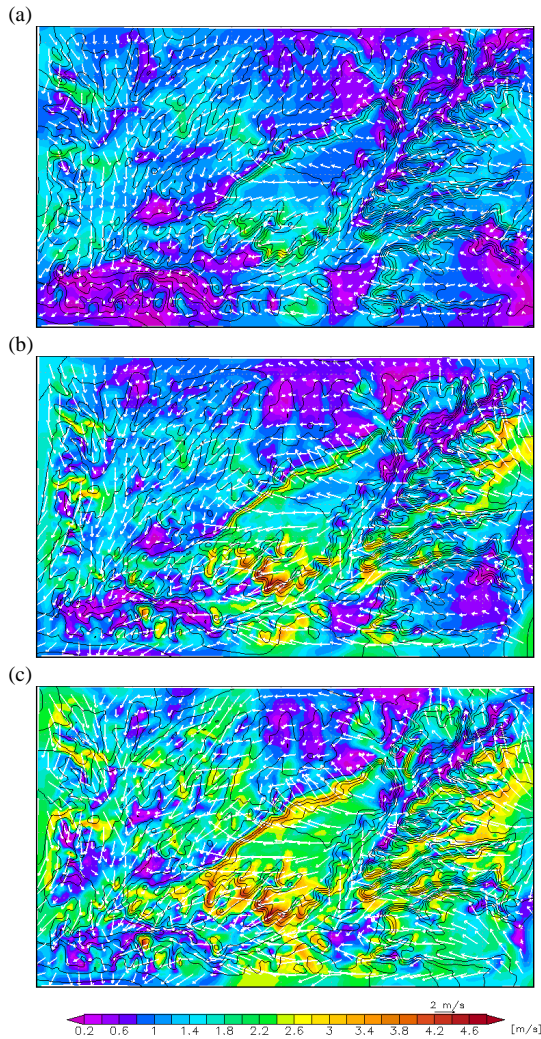


Figure 2. Simulated horizontal wind field for the inner domain at 10 m (AGL) by (a) MM5, (b) WRF-MYJ and (c) WRF-QNSE at 0400 UTC during the night of 14-15 January 2003.

The results show that the WRF model configurations tend to yield stronger winds, mainly in steep terrains, than those given by the MM5 model. To explain this model behaviour we must refer to the momentum equation for drainage flow over a sloping terrain. For low TKE values, such as those prescribed in WRF configurations, the effect of the buoyancy term that is supposed to be the source of the drainage flow is confined to a thin layer and its magnitude is increased. In contrast, the divergence of vertical flux related to the surface drag and the entrainment is decreased, which leads to a more realistic prediction of drainage flows in a thin layer, especially in the lower part of the mountainous areas. For higher TKE values, such as those prescribed by the MM5 model, the buoyancy term acts over a deep layer while the dissipation term or the divergence of vertical flux is increased, which leads to weaker drainage winds. An analysis of the spatial distributions of vertical temperature differences between 20 m and 2 m confirms that these differences are greatest over the steep terrain. The differences decrease over the Montes Torozos plateau, where the CIBA is located. However, in this area, WRF options also forecast higher winds than those forecasted by MM5, mainly for the QNSE scheme.

3.2 Temporal and vertical variations within the boundary layer

The simulations discussed in the previous sections were compared with measurements from the CIBA 100 m tower (Figure 3), which could be representative of the inner domain. Tower measurements showed the development of a low-level jet (LLJ) between 2300 and 0400 UTC (Figure 3a), which was fairly well captured by WRF-QNSE in terms of wind speed, but missed by MM5 and WRF-MYJ, probably due to the excessive vertical mixing caused by the imposed minimal TKE values of 0.2 ms^{-1} and 0.1 ms^{-1} respectively.

There were some errors in wind direction, as shown in Figure 3b, especially up to midnight, as very weak winds in the stable BL were highly erratic and sensitive to small and very local features. The models generated a steadier flow regime as they tended to smooth the representation of heterogeneities.

Another source of error could be that the incorrect distribution of near-surface temperatures produced an erroneous horizontal pressure gradient. At all levels, the observations showed a continuous clockwise turning of the wind until 0000 UTC (faster than corresponds to an inertial oscillation) and then constancy of direction when the LLJ was well developed. Although neither of the models captured the turning of the wind, the direction was fairly well represented by both of them at a later stage, thus indicating that the topographical influence that reached the CIBA was simulated by all models. The TKE evolution (not seen) was clearly overestimated by MM5 and WRF-MYJ, whereas WRF-QNSE was close to the observed values.

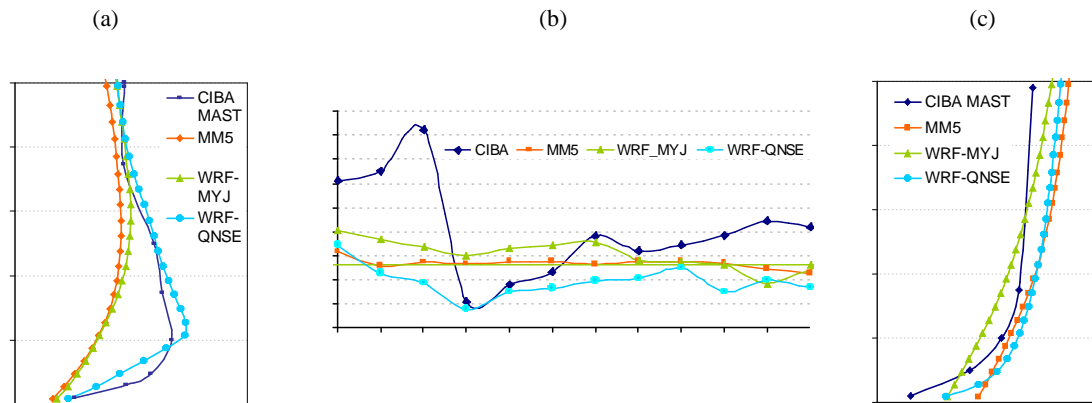


Figure 3. Comparison between simulated and measured values during the night of 14-15 January 2003 for the following: (a) vertical profiles of wind speed at 0400 UTC, (b) time series of wind direction at 10 m, (c) vertical profiles of potential temperature at 0100 UTC.

The potential temperature (Figure 3c) showed cold advection in the upper layers of the tower that was not observed in any of the models. Near the surface, models gave good estimations of the 2 m temperature, but MM5 tended to overmix the lower layers, whereas WRF, and particularly WRF-QNSE, maintained surface inversion and near-surface stability. In addition, there were no problems of excessive “runaway” cooling, since the QNSE scheme provided enough vertical turbulent transport, prescribing a TKE_{MIN} of $0.01 \text{ m}^2 \text{ s}^{-2}$.

To further evaluate the models’ performance, we used hourly averaged values measured by the tower at all levels for statistical analysis. Table 2 presents statistical values corresponding to the MM5 and WRF configurations indicated in Table 1

Table 2. Statistical values corresponding to MM5 and WRF model configurations.

Height		Statistic	Temperature ($^{\circ}\text{K}$)			Wind velocity (ms^{-1})			Wind direction (deg)		
T	WV-WD		MM5	WRF-MYJ	WRF-QNSE	MM5	WRF-MYJ	WRF-QNSE	MM5	WRF-MYJ	WRF-QNSE
2m	10m	MB	3.14	-0.62	0.43	-1.44	-0.35	-0.94	-25.95	3.66	-56.27
		MAGE	3.14	0.64	0.55	1.44	0.47	0.97	69.11	67.78	73.84
		RMSE	3.15	0.78	0.71	1.46	0.56	1.05	82.7	80.14	86.68
10m	20m	MB	0.70	-0.21	0.51	-1.46	-1.0	-0.58	5.65	-6.41	-1.83
		MAGE	0.70	0.41	0.82	1.46	1.0	0.68	61.78	73.82	73.49
		RMSE	0.83	0.49	0.86	1.5	1.07	0.82	74.09	85.03	86.05
20m	35m	MB	0.30	-0.34	0.48	-1.60	-1.04	-1.00	-10.46	-3.36	0.373
		MAGE	0.36	0.70	0.70	1.60	1.04	1.04	63.51	69.82	69.85
		RMSE	0.56	0.84	0.81	1.67	1.10	1.20	77.80	82.80	83.03
35m	50m	MB	0.30	0.46	0.36	-1.45	-0.86	-1.14	3.06	6.98	9.51
		MAGE	0.42	0.70	0.60	1.45	0.86	1.14	56.47	68.83	67.31
		RMSE	0.54	0.86	0.70	1.60	0.97	1.41	68.47	82.49	81.95
98m	75m	MB	-0.83	0.53	0.52	-1.24	-0.68	-1.06	-3.19	23.20	3.30
		MAGE	0.84	0.48	0.54	1.24	0.68	1.07	58.52	68.61	73.75
		RMSE	0.92	0.61	0.70	1.43	0.82	1.30	71.43	83.38	90.70
----- ---	98m	MB				-0.88	-0.35	-0.72	12.90	12.85	36.09
		MAGE				0.98	0.51	0.84	59.65	76.65	75.74
		RMSE				1.15	0.64	1.00	75.31	98.72	95.21

4. DISTRIBUTION OF POLLUTANTS UNDER NOCTURNAL THERMAL CIRCULATIONS

To study the 3D distribution of pollutants under nocturnal thermal conditions, MM5 and WRF options were coupled to the photochemical model CMAQ. Pollutants were emitted continuously from a virtual source located 20 m above ground level on the CIBA site, from 0000 UTC to 2400 UTC. The pollutant used in this work was SO_2 , with a chosen emission rate of 2537 t year^{-1} . The signature of the nocturnal thermal circulations on the horizontal distribution of SO_2 mixing ratios in the CIBA area was illustrated and analyzed by representing maps of concentrations and horizontal wind fields at (20 m a.g.l.). SO_2 dispersion patterns simulated by the three experiments agreed with the corresponding wind patterns discussed in Section 3.1. Thus, as all models forecasted downslope drainage winds from the Cantabrian mountain range in the bigger domain and wind from the E-SE in the inner domain, dispersion pattern differences were not very noticeable. However, as the WRF model configurations tended to yield stronger winds than those given by the MM5 model, particularly in steep terrains, higher SO_2 concentrations were found near these areas, as can be seen in Figure 4. Plume dispersion temporal analysis indicates that, early in the night, the MM5 and WRF model configurations transported SO_2 in minor and major intensity respectively to the north and northwest part of the inner domain. This is due to the presence of drainage winds in the steep terrain, which afterwards will be transported by the drainage winds coming from the northeast part of the inner domain. This previous analysis indicates that further study of the CMAQ model is required to predict pollutant concentrations in each case of the meteorological inputs from the above experiments.

5. CONCLUSIONS

In this study, two meteorological mesoscale models, MM5 and WRF, using different PBL schemes (ETA in MM5 and MYJ and QNSE in WRF) were run over the Duero basin in the Iberian Peninsula under very stable conditions. The models were compared and checked against available information from a 100 m meteorological tower. The results indicate that WRF provides more realistic meteorological predictions in the lower atmospheric region. In particular, a development of an LLJ was fairly well captured by the WRF-QNSE scheme. Both models were coupled to the CMAQ model to analyze the influence of the boundary layer parameterizations on air pollutant distribution and concentration. The results showed that the WRF in both configurations forecasted more effective transport than MM5, as it yielded stronger winds, mainly in steep terrains.

Acknowledgements

This research was supported by the Spanish Government in project CGL 2009- 12797-C03-02.

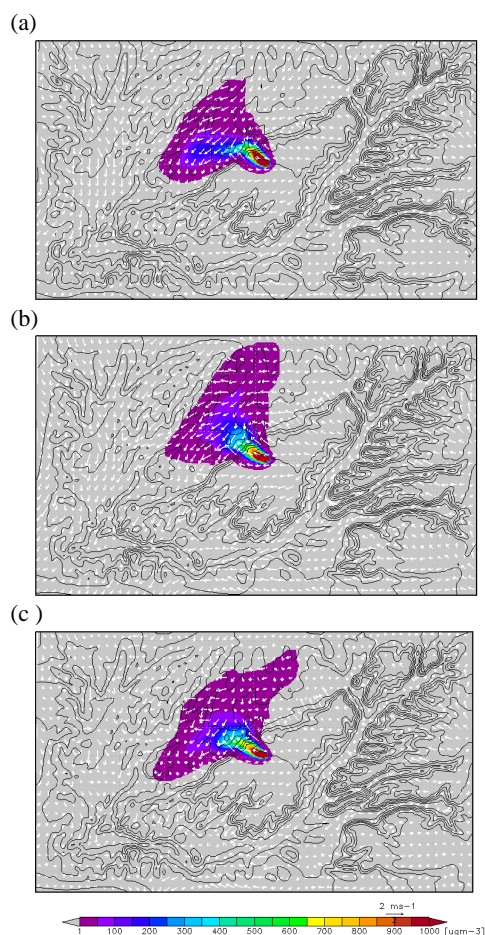


Figure 4. Maps of SO₂ concentrations and horizontal wind fields at 20 m and 0400 UTC, as simulated by (a) MM5 and CMAQ; (b) WRF-MYJ and CMAQ; (c) WRF-QMNSE and CMAQ.

REFERENCES

- Bravo, M. Mira, T. Soler, M.R. Cuxart, J., 2008: Intercomparison and evaluation of MM5 and Meso-NH mesoscale models in the stable boundary layer. *Boundary-Layer Meteorol.*, **128**, 77-101.
- Byung D.W., Ching, J.K.S. 1999: Science Algorithms of the EPA Models-3 Community Multiscale Air Quality (CMAQ) Modeling System. Environmental Protection Agency.
- Grell, GA, Dudhia, J. Stauffer, D R. 1994: A description of the fifth generation Penn State/NCAR Mesoscale Model (MM5). NCAR Tech. Note. NCAR/TN-398+STR
- Janjic, Z.I. 2002: Nonsingular implementation of the Mellor-Yamada Level 2.5 Scheme in the NCEP Meso model. NCEP Office Note 437, 61 pp. Available online at <http://www.ncep.noaa.gov>.
- Skamarock, W.C. Klemp, JB. Dudhia, J. Gill, DO. Barker, DM. Wang, W. Powers, JG. 2005: A description of the advanced research WRF version 2. NCAR Tech. Note NCAR/TN-468+STR, 88 pp.
- Sukoriansky, S. Galperin, SB. Perov, V. 2006: A quasi-normal scale elimination model of turbulence and its application to stably stratified flows. *Nonlinear Proc. Geophys.*, **13**, 9-22.
- Whiteman, C.D. 2000: Mountain Meteorology: fundamentals and applications. New York: Oxford University Press, pp141-236.